# Naturally occurring potentially toxic elements in groundwater from the volcanic landscape around Mount Meru, Arusha, Tanzania and their potential health hazard

Ines Tomašek [a,b,*], Hassina Mouri [c], Antoine Dille [b,d], George Bennett [e,f], Prosun Bhattacharya [g], Natacha Brion [a], Marc Elskens [a], Karen Fontijn [h], Yue Gao [a], Patrick Kirita Gevera [c], Julian Ijumulana [g,i], Mary Kisaka [b,j], Martine Leermakers [a], Ceven Shemsanga [j], Kristine Walraevens [e], Joanna Wragg [k], Matthieu Kervyn [b]

[a] Analytical, Environmental and Geochemistry (AMGC) group, Department of Chemistry, Vrije Universiteit Brussel, Belgium
[b] Physical Geography (FARD) group, Department of Geography, Vrije Universiteit Brussel, Belgium
[c] Department of Geology, University of Johannesburg, South Africa
[d] Department of Earth Sciences, Royal Museum for Central Africa, Tervuren, Belgium
[e] Laboratory for Applied Geology and Hydrogeology, Department of Geology, Ghent University, Belgium
[f] Department of Mining and Mineral Processing Engineering, University of Dodoma, Tanzania
[g] KTH-International Groundwater Arsenic Research Group, Department of Sustainable Development, Environmental Science and Engineering, KTH Royal Institute of Technology, Sweden
[h] Laboratoire G-Time, Department of Geosciences, Environment and Society, Université libre de Bruxelles, Belgium
[i] DAFWAT Research Group, Department of Water Resources Engineering, College of Engineering and Technology, University of Dar es Salaam, Tanzania
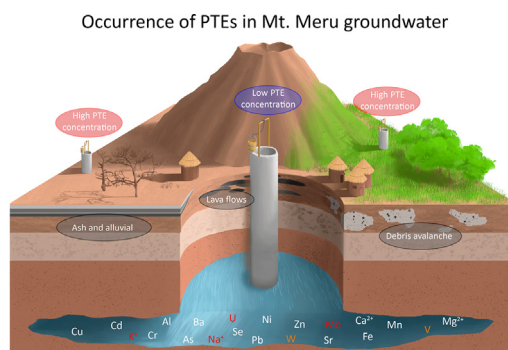[j] Department of Geology, University of Dodoma, Tanzania
[k] British Geological Survey, Environmental Science Centre, Nottingham, United Kingdom

## HIGHLIGHTS

- Population of Mt. Meru (in EARV) is facing issues with water scarcity and quality.
- We assess the presence of potentially toxic elements (PTE) in groundwater sources.
- In some of the samples, concentrations of Mo and U exceed the permissible limits.
- Other analysed PTEs are within the acceptable limits for drinking purpose.
- The areas of high concentrations are covered with debris avalanche and ash deposits.

## GRAPHICAL ABSTRACT

**ABSTRACT**

The population of the semi-arid areas of the countries in the East African Rift Valley (EARV) is faced with serious problems associated with the availability and the quality of the drinking water. In these areas, the drinking water supply largely relies on groundwater characterised by elevated fluoride concentration (> 1.5 mg/L), resulting from interactions with the surrounding alkaline volcanic rocks. This geochemical anomaly is often associated with the presence of other naturally occurring potentially toxic elements (PTEs), such as As, Mo, U, V, which are known to cause adverse effects on human health. This study reports on the occurrence of such PTEs in the groundwater on the populated flanks of Mt. Meru, an active volcano situated in the EARV.

Our results show that the majority of analysed PTEs (Al, As, Ba, Cd, Cr, Cu, Fe, Mn, Ni, Se, Sr, Pb, and Zn) are within the acceptable limits for drinking purpose in samples collected from wells, springs and tap systems, suggesting that there is no immediate health risk associated with these PTEs. However, some of the samples were found to exceed the WHO tolerance limit for U (> 30 μg/L) and Mo (> 70 μg/L). The sample analysis also revealed that in some of the collected samples, the concentrations of total dissolved solids, Na$^+$ and K$^+$ exceed the permissible limits. The concerning levels of major parameters and PTEs were found to be associated with areas covered with debris avalanche deposits on the northeast flank, and volcanic ash and alluvial deposits on the southwest flanks of the volcano. The study highlights the need to extend the range of elements monitored in the regional groundwater and make a more routine measurement of PTEs to ensure drinking water safety and effective water management measures.

## 1. Introduction

Globally, numerous studies provide evidence of the contamination of groundwaters with naturally occurring potentially toxic elements (PTEs), including, but not limited to, arsenic (As), cadmium (Cd), chromium (Cr), copper (Cu), molybdenum (Mo), nickel (Ni), lead (Pb), uranium (U) and vanadium (V) (Nwankwo et al., 2020; Bundschuh et al., 2017; Mitchell et al., 2011). The occurrence of such elements in groundwater is highly dependent on the local geological background and climate, as they are principally released through water-rock interactions and weathering (*e.g.*, Rango et al., 2009). These processes are governed by the PTE abundance and chemical state in the rocks as well as physicochemical properties of groundwater. Additionally, human activities including mining and agriculture can also contribute to the release of PTEs into the environment (Bundschuh et al., 2017). The presence of such elements in groundwater, in excessive amounts, is associated with adverse human health impacts (*e.g.*, Muhammad et al., 2011; Ormachea Munoz et al., 2013; Rahman et al., 2015). Each PTE has unique physicochemical properties and specific mechanisms of toxicity. Yet, in general, they have been reported to impact the biological function and cause cellular and tissue damage leading to a variety of adverse effects and diseases (Edmunds and Smedley, 1996; Wang and Shi, 2001; Tchounwou et al., 2012). Notably, excess or deficiency of some essential elements in drinking water, like fluoride (F$^-$), iodine (I) and selenium (Se), can lead to serious health issues such as dental or skeletal fluorosis and thyroid enlargement or goiter (Gevera et al., 2019; Zimmermann, 2009; Fordyce, 2013).

Groundwater quality problems are a well-established feature of the East African Rift Valley (EARV). This area is a host of prominent tectonic activity, volcanism and associated hydrothermal systems which contribute to a large input of PTEs to the environment (Davies, 2008; Rango et al., 2009). In semi-arid areas of the countries in the EARV, like Ethiopia, Kenya and Tanzania, the most commonly reported issue is the occurrence of high concentrations of F$^-$ that exceed the World Health Organization (WHO) guideline of 1.5 mg/L in drinking water (Malago et al., 2017; Gevera and Mouri, 2018; Ijumulana et al., 2020). The main processes controlling the F$^-$ concentrations found in groundwater include interactions with the surrounding alkaline volcanic rocks and unconsolidated sediments, and evaporation (*e.g.*, Rango et al., 2009; Ghiglieri et al., 2010; Kimambo et al., 2019). Although it is known that high F$^-$ levels in such geological environments are often associated with the presence of other naturally occurring PTEs, such as As, Mo, U and V (Rango et al., 2010), only a limited number of studies have investigated and reported their presence, and in levels of health concern, in

the EARV groundwater (Gevera et al., 2020; Malago et al., 2020; Ijumulana et al., 2020, 2021; Mekonnen et al., 2012; Rango et al., 2010; Reimann et al., 2003). Considering that the exposure to such PTEs may potentially aggravate F$^-$ toxicity and, hence, increase the risk of adverse health effects (Chowdhury et al., 2016; Mitchell et al., 2011), there is a clear need to systematically assess their occurrence and levels in the groundwater in order to appropriately characterise the groundwater's quality and safety for use.

The focus of this study is groundwater quality on the flanks of Mt. Meru, an active volcano situated in the EARV, in the northern part of Tanzania (Fig. 1). Over one million people living in the surrounding of the volcano are faced with serious problems associated with the availability and the quality of water. The water supply largely relies on the groundwater wells, boreholes and springs, which is characterised in many places by F$^-$ concentration exceeding the local and international drinking water guidelines, resulting from the interactions with the surrounding volcanic deposits (Fig. 2) (Ghiglieri et al., 2012, 2010). Consequently, previous studies of water quality in the region have mainly focused on the F$^-$ geochemistry and associated health problems (dental and skeletal fluorosis) affecting the local population (Ijumulana et al., 2021; Makoba and Muzuka, 2019; Kitalika et al., 2018; Mbabaye et al., 2018; Chacha et al., 2018; Mkungu et al., 2014). However, little to no research is available on contamination by other naturally occurring PTEs in drinking water (Malago et al., 2020) and their possible health effects. Local communities use the water for drinking, domestic purposes, livestock keeping, agricultural (*i.e.*, irrigation) and industrial activities, but different water sources are often used without testing the suitability of water for specific uses.

The objective of this study is, therefore, to determine the concentrations and distribution of selected PTEs in groundwater, including As, Cd, Cu, Mo, Ni, Pb, Se, U and V, to provide this information on water quality, critically lacking in the study area, and the EARV in general. We sampled and analysed water from 48 sites used by local population including wells, springs and tap systems around Mt. Meru (Fig. 1), to assess its suitability for drinking and the potential health risk associated with its consumption. Additionally, using the existing geochemical data (from Bennett et al., 2021), we explored the relationship of analysed PTEs with F$^-$ and other physicochemical parameters in the groundwater as well as their spatial variability to delineate the areas of poor water quality and evaluate their association with the underlying geological units (Fig. 2).

## 2. Study area

The investigated area covers the flanks of Mt. Meru, situated in the Arusha region along the Eastern branch of the EARV, in northern
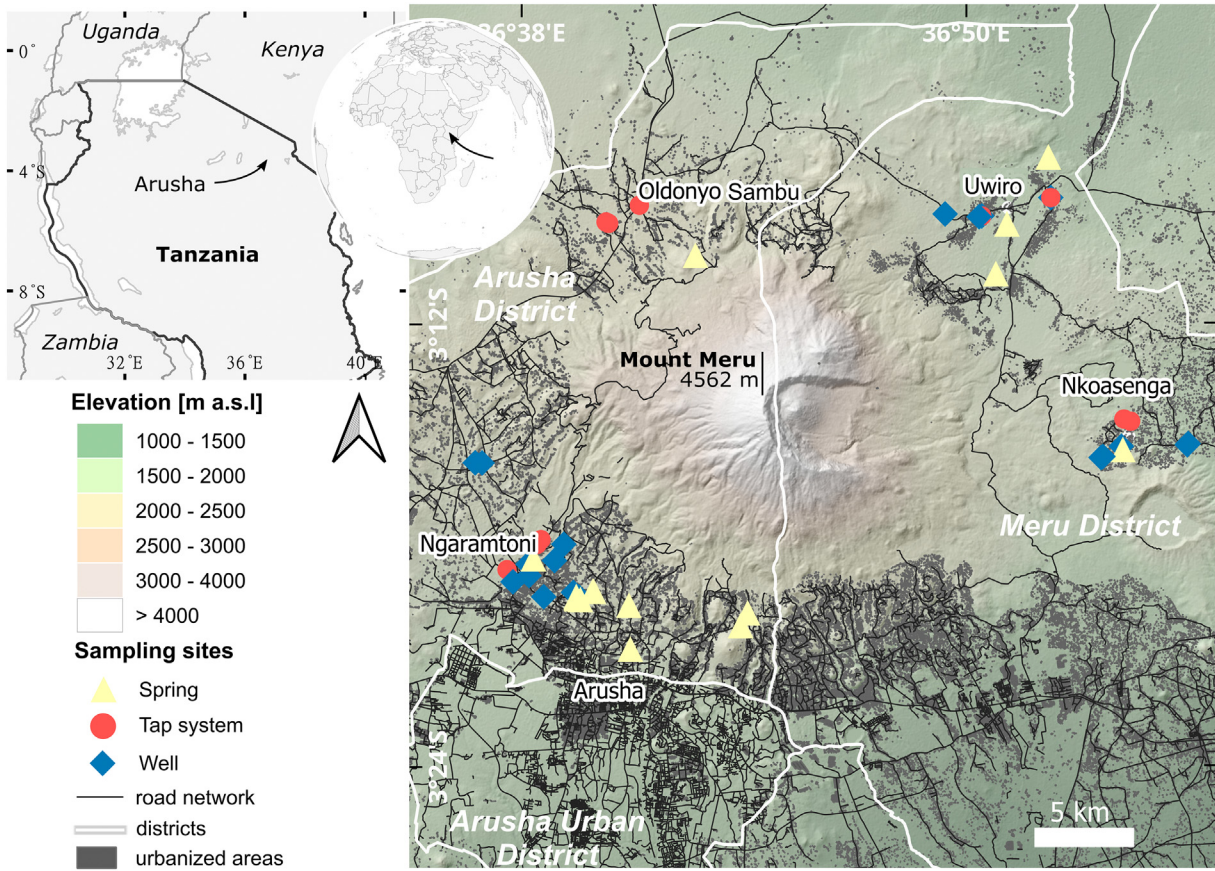
**Fig. 1.** Geographical map of the study area around Mt. Meru in the Arusha region in northern Tanzania. The map indicates surface elevation, regional district boundaries, main settlements, and the water sampling locations according to the type (wells, springs and tap water).

Tanzania (Fig. 1). The population of the region has been estimated to approximate 1.7 million people (United Republic of Tanzania Census 2012). The majority are concentrated in Arusha city on the southern flanks of the volcano (Arusha City district having 416,442 inhabitants), but there is a distributed rural population on all the flanks with respectively 323,198 and 268,144 inhabitants in the Arusha and Meru districts,
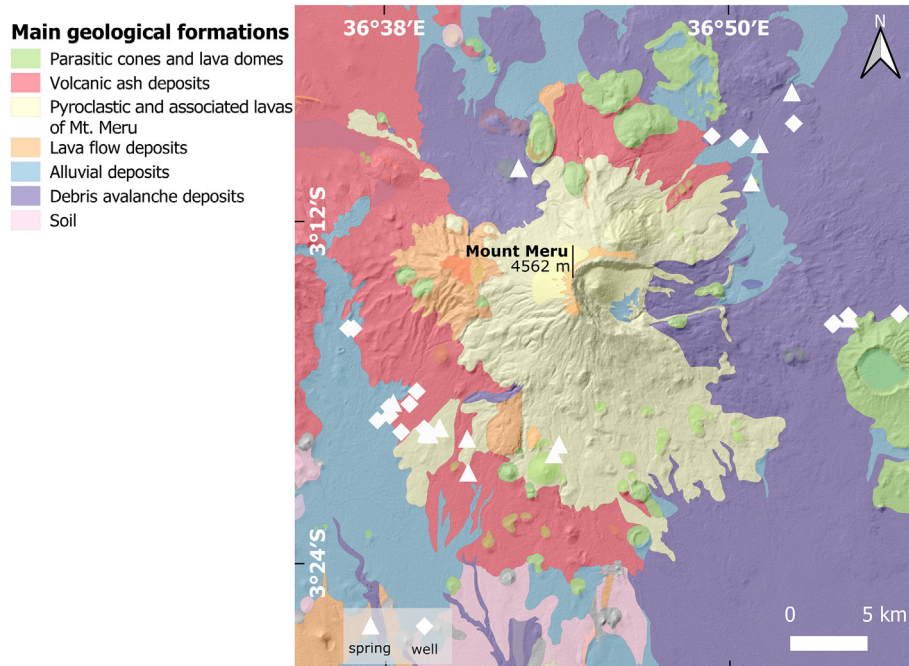


**Fig. 2.** Simplified geological map of the study area, indicating different lithologies. The map was digitized based on the geological map of Arusha (Geological Survey of Tanzania, 1983) with updates from Delcamp et al. (2017).

which cover most parts of the study area (Fig. 1). The Arusha district has a population density of 261 persons per km² and the Meru district of 212/km². That is approximately four to five times higher than the regional and national population density of 45/km² and 51/km², respectively (United Republic of Tanzania Census, 2012). In the study area, the population density is lowest in the arid western flank, which coincides with the area blanketed by voluminous tephra fallout (pumice and ash) and reworked deposits (Kisaka et al., 2021).

The topography of the study area (Fig. 1) is dominated by the steep slopes of Mt. Meru (4562 m a.s.l) which divides the area into two climatic zones - windward and leeward side (Makoba and Muzuka, 2019). The rainfall is irregularly distributed between a main wet season characterised by long rains (February – May) and a minor one with short rains (October – December). The average annual rainfall is 500 mm or less for areas at low (< 1400 m) elevation and in the leeward zone, whereas the windward side and areas at high (> 1400 m) elevations receive around 1200 mm (Chacha et al., 2018; Makoba and Muzuka, 2019). The temperatures range between 13 and 30 °C with an annual average of about 25 °C (Chacha et al., 2018).

The lithology of the study area is characterised by various volcanic deposits (Fig. 2), predominantly of nephelinite and phonolite compositions, including debris-avalanche deposits, lava flows, pyroclastic density current deposits, pumice and ashfall deposits, with some alluvial sediments (Kisaka et al., 2021; Delcamp et al., 2017; Ghiglieri et al., 2010; Roberts, 2003; Wilkinson et al., 1986). These rocks of varying permeabilities form aquifers with different mineralogical compositions with some of the minerals potentially being a host to considerable concentrations of PTEs (e.g., biotite, muscovite, apatite) (Davies, 2008).

Groundwater access in the study area is through hand- or machine-dug wells (depth range between 0.7 and 50 m), springs and boreholes (depth range between 48 and 170 m) (Bennett et al., 2021). Some wells are drilled close to cowsheds and pit latrines, which can contribute to water quality deterioration (Makoba and Muzuka, 2019). Moreover, the main anthropogenic activities in the area are agriculture (e.g., corn, beans, coffee, and fruits) and livestock keeping which can also lead to groundwater contamination and increased water scarcity in some areas.

The water sources investigated in this study are distributed across the area in roughly four clusters (Fig. 1); one in the southwest in the Ngaramtoni village and surroundings, one in the northwest around the Oldonyo Sambu ward, one in the northeast in the Uwiro village and one in the east near the Nkoasenga village. Some springs at higher elevations are being tapped at and redistributed to areas at lower elevations through a piped network and tap installations, making the water available to local communities. However, limited data is available on the locations of springs or boreholes that are being tapped and on the extent of this system, which is rather scattered across the study area.

## 3. Materials and methods

### 3.1. Water sampling

Our sampling campaign took place in August 2018, during the dry season. Water samples for the analysis of major (Ca, Na, K, Mg) and PTEs (Al, As, Ba, Cd, Co, Cr, Cu, Fe, Mn, Mo, Ni, Pb, Se, Sr, U, V, W, Zn) were collected from 48 sites, including 19 wells, 18 springs and 11 tap systems (Fig. 1). The sampling points were selected to include drinking water sources, and those used for domestic and agricultural purposes. They were thus constrained by the availability of groundwater and were distributed across the area in locations in proximity to settlements, hence, the uneven sampling coverage pattern. Furthermore, the sources on the southern and southeastern flanks were not investigated. Sample location information (coordinates and altitude; Appendix 1) were recorded in the field using a handheld eTrex 20 GPS (Garmin, USA).

### 3.2. Analytical methods

Physicochemical parameters including pH, temperature and electric conductivity (EC; Appendix 1) were measured in situ using a portable multiparameter water monitoring probe AP-2000 (Aquaread, UK). Samples were filtered onsite using a 0.45 μm filter, acidified with nitric acid (HNO₃ 69% AR/ACS Loba Chemie) and stored in 15 mL polyethylene (centrifuge) tubes. They were then transported to Belgium and analysed at the facilities of the AMGC research group of the Vrije Universiteit Brussel.

High-resolution inductively coupled plasma mass spectrometry (HR-ICP-MS) analyses to determine the concentrations of major (Ca, Na, K, Mg) and PTEs (Al, As, Ba, Cd, Co, Cr, Cu, Fe, Mn, Mo, Ni, Pb, Se, Sr, U, V, W, Zn) were carried out using the Element II spectrometer (Thermo Finnigan, USA). Quantitative determinations were conducted by external calibration with a multi-elements standard solution using $^{103}$Rh as an internal standard to correct instrumental drift and to assess the instrumental accuracy and precision. The analytical precision was established by multiple standard and sample measurements, and accuracy by the analysis of reference materials (NRCC, river water SLRS6).

The anions could not be analysed in our samples since they were treated (acidified) to preserve the metals. Hence, we used data from Bennett et al. (2021) on F⁻, chloride (Cl⁻), sulphate ($SO_4^{2-}$), nitrate ($NO_3^-$), bicarbonate ($HCO_3^-$) and phosphate ($PO_4^{3-}$) concentrations for samples collected in some of the investigated sites in the same period (August–September 2018). This allowed us to compile datasets for our statistical and spatial analyses to contextualise the PTE concentrations determined in this study (see Appendices 2 and 3). We refer the reader to Bennett et al. (2021) for the overview of the general groundwater quality in the study area and a detailed description of the different analytical methods used to determine anion concentrations.

### 3.3. Data analyses

#### 3.3.1. Groundwater quality assessment

The chemical composition of the studied water samples was compared to the recommended guidelines set by the World Health Organization (WHO, 2017) and the Tanzania Bureau of Standards (TBS; in Tanzania Standard (TZS) 789:2008) for drinking water. The data (available in Appendix 1) are summarised for the whole study area (n = 48; in Table 1) and separately reported for the subsets of samples (tap system, wells and springs; in Figs. 3 and 4) given their different origin (i.e., type of water source). The analysis of the statistical distributions of the data (Shapiro-Wilk test at 0.05 significance level) showed that most parameters, except for pH and As, were not normally distributed (i.e., not following a Gaussian distribution). Hence, the statistical significance of the measured concentrations of PTEs among the different water sources was deduced through the use of a Kruskal-Wallis test with subsequent Dunn's multiple comparisons tests (α = 0.05). Graphical representation and statistical analyses of the data were performed using the GraphPad Prism software (version 9.0.0).

#### 3.3.2. Health risk assessment

To assess the exposure to PTEs via oral pathway and to estimate potential health risk associated with consumption of water with elevated concentrations of PTEs, chronic daily intake (CDI, in mg/kg/day) was calculated according to the following equation (Eq. (1)):

$$CDI = \frac{C \times IR}{BW} \tag{1}$$

where C is the concentration of PTE in water (mg/L), IR is the average daily intake rate (1 L/day for children and 2 L/day for adults (WHO, 2003)) and BW is the average body weight (20 kg for children and 70 kg for adults).

The probability of non-carcinogenic risk posed by a PTE was then estimated based on the calculation of hazard quotient (*HQ*) as follows (Eq. (2)):

$$HQ = \frac{CDI}{RfD} \tag{2}$$

where *RfD* is the oral reference dose of PTE (mg/kg/day), obtained from the database of United States Environmental Protection Agency's (US EPA) Integrated Risk Information System (IRIS; *www.epa.gov/iris*). If the ratio is found to be less than 1, it is assumed that no appreciable risk of harmful effects occurring during a lifetime is expected.

### 3.3.3. Multivariate analysis

Principal component analysis (PCA) was used to deduce the key physicochemical parameters that characterise the groundwater in the study area. This technique reduces the original data into a new set of interrelated variables (principal components, PCs) which best describe the variation present in the dataset (Wold et al., 1987). The analysis was based on a correlation matrix (standardized data scaled to have a mean of 0 and SD of 1) and the PCs were selected based on the eigenvalues greater than 1.0 ("Kaiser rule"). The PCA also allowed us to evaluate the relationships of selected PTEs with $F^-$ and the dominant water parameters as well as to determine the clusters of water sources with similar hydrochemical characteristics by plotting the sample PC scores.

Groundwater samples were not split into groups for this assessment, so the data included parameters for 28 sites (17 wells and 11 springs) investigated in this study for which a full physicochemical information was available (*i.e.*, by combining our cation and PTE data with that of anions from Bennett et al. (2021) for these locations; see Appendix 2).

### 3.3.4. Spatial distribution analysis

The inverse distance weighting (IDW) interpolation method (as per Quino Lima et al., 2020) was used to generate maps showing the spatial variation of selected PTE concentrations and other parameters in the groundwater across investigated wells and springs. Tap system samples were omitted from this analysis as the source locations are typically uncertain or unknown. Hence, the interpolation for PTEs was done based on the data acquired in this study for 37 sampling points in the study area (~2000 km²). To depict the distribution of water dominant ions ($F^-$, $Cl^-$, $HCO_3^-$, $SO_4^{2-}$, Na, K) we used the extended dataset for water samples collected in August/September 2018 from Bennett et al. (2021) for 62 locations (of which 28 correspond to our sampling points; Appendix 3).

## 4. Results

### 4.1. Groundwater quality in the study area

The statistical summary of the water quality parameters and their variation for all analysed samples across the different water sources is listed in Table 1.

### 4.1.1. Physicochemical characteristics

The groundwater in the study area is, on average, circumneutral to slightly alkaline (mean of pH 7.5) with values found below the TBS guidelines (up to 9.2) and within the acceptable WHO range of 6.5 to 8.5 in all analysed water sources (Fig. 3, Table 1). The highest average value (pH 8) and lowest variation, which significantly differed ($p < 0.05$) from pH measured in other sources, were recorded in tap water (Fig. 3). The highest variability in pH was observed in water from springs. Total dissolved solids (TDS), derived from the measured EC, were the lowest in tap water with an average value of 460 mg/L, and were most variable in water from springs, reaching values of >2000 mg/L (Fig. 3). On average, the palatability of water from wells and springs was found to be poor (> 500 mg/L; Table 1), however, only 7% ($n = 3$) of the analysed samples exceeded the recommended WHO limit of 1500 mg/L (Fig. 3). These include two springs which also exceeded the limit set by TBS of 2000 mg/L.

### 4.1.2. Major element characteristics

The concentrations of major elements were found to be in order of dominance as $Na^+ > K^+ > Ca^{2+} > Mg^{2+}$ and were largely comparable across the water sources, with their lowest concentrations measured in tap water (Fig. 3). Mean Na concentration was 200 mg/L (Table 1), corresponding to the WHO limit which was exceeded in 31% ($n = 15$) of all

**Table 1**
Descriptive statistics (range, median, mean, standard deviation) of the measured parameters in groundwater for the total of 48 samples in the study area. The data were compared to the recommended drinking water guidelines set by the World Health Organization (WHO, 2017) and the Tanzania Bureau of Standards (in TZS 789:2008). The values exceeding the WHO limit are in bold. All parameters, except for TDS in two samples, were below the (available) TBS guideline values.

| Parameter | # | Minimum | Median | Maximum | Mean | SD | WHO (2017) | % above WHO | TBS (2008) |
|---|---|---|---|---|---|---|---|---|---|
| pH | 44 | 6.6 | 7.6 | 8.5 | 7.5 | 0.5 | 6.5–8.5 | | 6.5–9.2 |
| mg/L | | | | | | | | | |
| TDS | 44 | 123 | 578 | **2014** | 663 | 415 | 1500 | 7 | 2000 |
| Ca | 48 | 2 | 22 | **119** | 24 | 20 | 100 | 2 | 300 |
| K | 48 | 5 | 39 | **114** | 40 | 23 | 50 | 23 | n/a |
| Na | 48 | 11 | 144 | 868 | **200** | 185 | 200 | 31 | n/a |
| Mg | 48 | 0.2 | 3.9 | 10.0 | 3.9 | 2.8 | 100 | | 100 |
| | | | | | | | | | |
| µg/L | | | | | | | | | |
| Al | 47 | 0.1 | 0.2 | 5.1 | 0.6 | 1.0 | 200 | | n/a |
| Cu | 48 | 0.2 | 1.6 | 6.6 | 1.9 | 1.5 | 2000 | | 3000 |
| Fe | 48 | 2 | 10 | **497** | 35 | 77 | 300 | 2 | 1000 |
| Mn | 48 | 0.1 | 1.0 | 181.0 | 6.5 | 26.0 | 400 | | 500 |
| Zn | 48 | 0.5 | 1.6 | 97.0 | 6.9 | 16.0 | 1500 | | 15,000 |
| As | 48 | 0.1 | 1.7 | 4.9 | 1.8 | 1.5 | 10 | | 50 |
| Ba | 48 | 0.5 | 5.2 | 35.0 | 11.0 | 11.0 | 700 | | 1000 |
| Cd | 48 | 0.01 | 0.07 | 1.10 | 0.15 | 0.27 | 3 | | 50 |
| Cr | 48 | 0.03 | 0.15 | 1.80 | 0.32 | 0.41 | 50 | | 50 |
| Mo | 48 | 2 | 27 | **722** | **82** | 173 | 70 | 13 | n/a |
| Ni | 48 | 0.02 | 0.08 | 0.74 | 0.13 | 0.16 | 20 | | n/a |
| Pb | 48 | 0.04 | 0.06 | 1.10 | 0.11 | 0.16 | 10 | | 100 |
| Se | 48 | <0.01 | 0.95 | 7.10 | 1.70 | 1.70 | 10 | | 50 |
| Sr | 48 | 47 | 371 | 1402 | 440 | 339 | 4000 | | n/a |
| U | 48 | 0.1 | 4.2 | **92.0** | 14.0 | 19.0 | 30 | 25 | n/a |
| V | 48 | 0.6 | 15.0 | 54.0 | 18.0 | 13.0 | n/a | | n/a |
| W | 48 | 1 | 82 | 418 | 110 | 106 | n/a | | n/a |
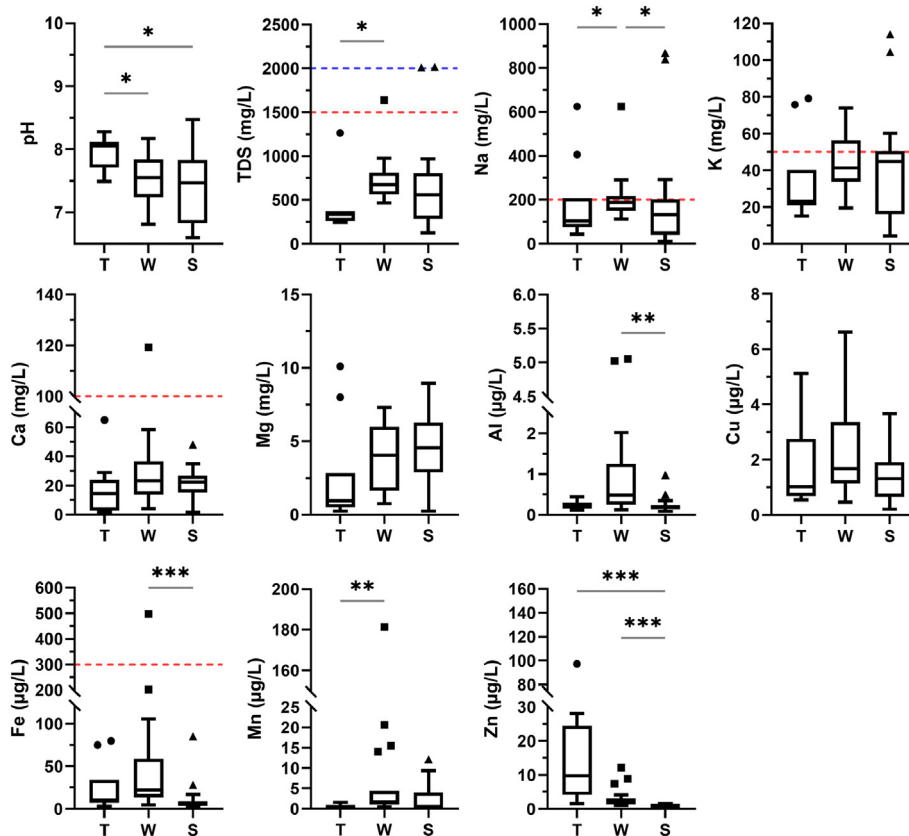
Fig. 3. Boxplots for distribution of major cations (Ca, K, Na, Mg) and elements affecting the taste, odour and appearance of drinking water across the different water sources in Mt. Meru area. The sources are indicated as T – tap system ($n = 11$), W – wells ($n = 19$), and S – springs ($n = 18$). The red dashed line indicates the WHO recommended level in drinking water for the parameter. The blue dashed line indicates the TBS recommended level in drinking water for the parameter. The absence of the dashed line means either that the threshold value is not established, or it exceeds the range of the graph. The statistical significance is denoted according to P values as 0.033 (*), 0.002 (**), < 0.001 (***).

samples, while K was found to exceed the recommended limits in 23% ($n = 11$) of the samples. These elements are not regulated on a national level. Concentrations of Ca were below the TBS limit (300 mg/L) in all samples, and below the WHO limit (100 mg/L) except in one well sample where the maximum value of 119 mg/L was recorded (Table 1). Magnesium was found to be well below the recommended values of 100 mg/L in all samples, with maximum measured concentration of only 10 mg/L (Table 1).

### 4.1.3. PTE characteristics

The elements, which are considered PTEs but mainly affect the taste, odour and visual appearance of water, namely Al, Cu, Fe, Mn and Zn, were found in acceptable concentrations in all samples, and below their taste or health-based WHO guidance values, except for Fe in one well sample exceeding the WHO limit of 300 μg/L with its concentration measured at 497 μg/L (Table 1). All were also below their respective limits set by TBS (Table 1). On average, the concentrations of these elements were higher and more variable in water from wells, except for Zn, which was significantly higher ($p < 0.05$) in tap system water (Fig. 3). With regards to other analysed PTEs, there was no statistically discernible difference ($p > 0.05$) in mean concentrations of As, Cd, Cr, Mo, Se, Sr and V among the different sources (Fig. 4). Pb was notably higher ($p < 0.05$) in the tap system water and Ni in well water (Fig. 4) compared to other sources. The concentrations of As, Ba, Cd, Ni, Pb, Se and Sr in the analysed samples were generally low and did not exceed available national or international standards for drinking water (Table 1). According to the WHO, there are no established health-based limits for V and W, but their average concentrations of 18 μg/L and 110 μg/L, respectively (Table 1), can be characterised as high based on some

typical values reported in the literature (Gerke et al., 2010; Steenstra et al., 2020). The concentrations of Mo and U were found to be above the provisional limits suggested by WHO for drinking water of 70 and 30 μg/L (Fig. 4), in 13% ($n = 6$) and 25% ($n = 12$) of samples among all water sources, respectively.

### 4.2. Health risk assessment from exposure to PTEs

The chronic daily intake (CDI) of PTEs via water consumption and associated hazard quotients (HQs) were only calculated for Mo and U since they were the only investigated PTEs found at elevated concentrations. The oral reference doses (RfD) used were $5 \times 10^{-3}$ and $6 \times 10^{-4}$ mg/kg/day for Mo and U, respectively (US EPA, Gilman et al. (1998)). For the samples where Mo exceeded 500 μg/L (MW20, MW21, MW23 and MW24), the HQs were found to be high (>1) for both adults and children, whereas Mo concentration of around 100 μg/L (sample MW49) represents risk only for children (Appendix 4). The HQs for the sample with concentration of Mo at the health limit (70 μg/L; MW40) were < 1. All 12 samples where U exceeds the WHO limit of 30 μg/L (Appendix 4) had high HQs (>1), for both adults and children. In addition, samples where U concentration was around 18 μg/L (MW25 and MW40) indicate HQ >1 for children (Appendix 4).

### 4.3. Relationships between PTEs and dominant parameters in the groundwater

#### 4.3.1. Principal components

From the 29 analysed parameters, PCA identified seven principal components (PC) with eigenvalues greater than 1.0 (Appendix 2),
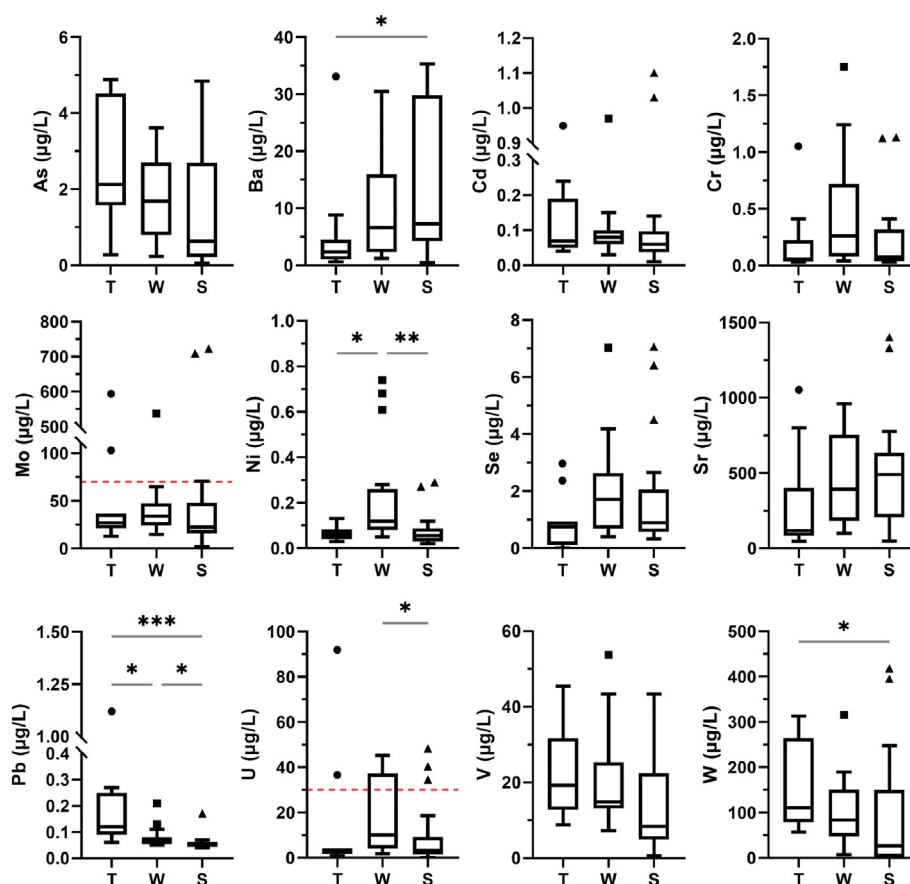
**Fig. 4.** Boxplots for the concentrations of potentially toxic elements (PTEs) in drinking water across the different water sources in Mt. Meru area. The sources are indicated as T – tap system (n = 11), W – wells (n = 19), and S – springs (n = 18). The red dashed line indicates the WHO recommended level in drinking water for the parameter. The absence of the red dashed line means either that the threshold value is not established, or it exceeds the range of the graph. The statistical significance is denoted according to P values as 0.033 (*), 0.002 (**), < 0.001 (***).

with three key PCs (PC1 – PC3) cumulatively explaining 65.5% of the variation in groundwater chemistry (Table 2). The first PC accounted for 39.5% of the total variance within the dataset and was dominated by TDS, Na, $Cl^-$, $SO_4^{2-}$, $HCO_3^-$, Cd and Mo with factor loading values greater than 0.9, and to a lesser extent with K, $F^-$, As, Cr, Se, Sr, U, V and W with loadings between 0.5 and 0.9 (Table 2). The second component (PC2) represented 16.7% of the total variance and was dominated by Mg and $NO_3^-$ (Table 2). Variables including pH, Ca and $PO_4^{3-}$ were positively correlated with the third component (PC3) which explained 9.3% of the total variance. Other constituents (*e.g.*, Cu, Mn, Ni, Zn) were not as well represented in PCA as indicated by the smaller factor loadings shown in the Table 2.

### 4.3.2. PCA correlation

The correlation between the variables and the factors (PC1 and PC2) is reported in Appendix 2 and graphically represented in Fig. 5a, which also indicates the degree of association between the variables (based on the angle of each vector relative to other vectors). Molybdenum was highly correlated with TDS, Na, K, $Cl^-$, $SO_4^{2-}$, $HCO_3^-$ and Cd ($r = 0.8–1.0$), and moderately with $F^-$, Ba, Se, Sr, V and W ($r = 0.5–0.8$) (Appendix 2). Uranium showed moderate correlation with TDS, Na, Ca, $HCO_3^-$, Cr, Se and Sr ($r = 0.5–0.8$). With respect to the other measured PTEs, $F^-$ was found moderately associated only with Cd, Mo and V ($r = 0.5–0.7$). In turn, concentrations of V were strongly positively correlated with pH, As and W ($r > 0.6$); all showed a negative association with $NO_3^-$ (Fig. 5a).

### 4.3.3. PCA sample clustering

Based on the factor scores for PC1 and PC2, the data for the 28 sample locations were projected as points on a biplot (Fig. 5b) which can

indicate samples that are similar in terms of their chemical signature. One prominent cluster is grouping of samples (wells MW41, MW42 and MW46, spring MW47) in quadrant 1, due in large part to high concentrations of Na, $HCO_3^-$ and U. Another cluster is illustrated by close grouping of samples of spring water (MW5, MW7, MW8, MW9) in quadrant 2, reflecting the lowest concentrations of dominant parameters and high $NO_3^-$. The most isolated points, *i.e.*, samples that do not cluster with others (well MW20, and springs MW23 and MW24) are positioned in the right-hand side of the biplot in quadrant 4. This quadrant is characterised by high concentrations of the dominant parameters, and these samples had the highest concentrations of all major ions observed throughout the studied locations (Appendix 1). The lack of clustering of other samples on the biplot indicates the variability in their chemical signatures (Fig. 5b).

### 4.4. Spatial distribution of major ions and PTEs in groundwater sources

The spatial distribution of some of the dominant physicochemical parameters in the groundwater and selected PTEs in the study area is shown in Figs. 6 and 7.

Major ions (Na, K, $HCO_3^-$, $Cl^-$, $SO_4^{2-}$), and associated TDS, showed similar distribution patterns with the highest concentrations of these parameters clustered in the northeast and southwest of the study area (Fig. 6), whereas a zone with their lowest concentrations was on the northwest flank of the volcano. A similar trend for areas of highest concentrations was observed for PTEs including U and Mo (Fig. 7). Moreover, high concentrations of $F^-$ (> 4 mg/L) were widely distributed across the study area as was the occurrence of concentrations considered high for V and W (Wright and Belitz, 2010; Hobson et al., 2020).

**Table 2**
Factor loadings of principal component analysis (PCA) for groundwater samples ($n = 28$) in the study area for the three main factors/components. The values in bold represent the dominant parameters (with factor loadings >0.4).

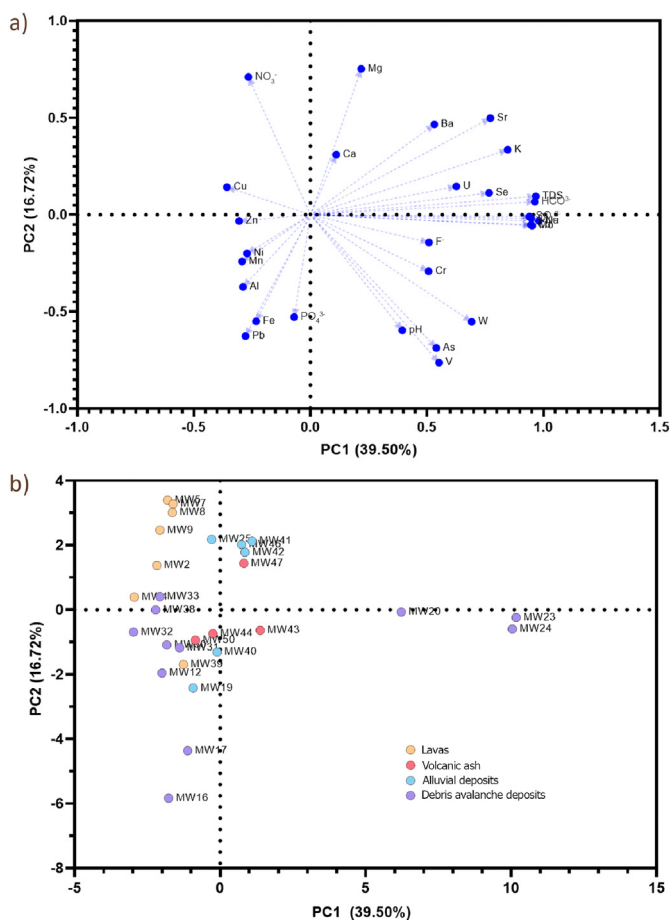| Parameter | PC1 | PC2 | PC3 |
|---|---|---|---|
| pH | 0.394 | **−0.596** | **0.471** |
| TDS | **0.967** | 0.095 | −0.006 |
| Ca | 0.110 | 0.310 | **0.442** |
| K | **0.846** | 0.335 | −0.132 |
| Na | **0.980** | −0.032 | −0.050 |
| Mg | 0.217 | **0.752** | −0.270 |
| F⁻ | **0.508** | −0.143 | −0.128 |
| Cl⁻ | **0.948** | −0.018 | −0.184 |
| SO₄²⁻ | **0.939** | −0.009 | −0.144 |
| NO₃⁻ | −0.267 | **0.710** | −0.004 |
| HCO₃⁻ | **0.963** | 0.067 | −0.023 |
| PO₄³⁻ | −0.069 | **−0.528** | **0.466** |
| Al | −0.290 | −0.372 | **−0.736** |
| Cu | −0.359 | 0.142 | −0.019 |
| Fe | −0.233 | **−0.549** | **−0.692** |
| Mn | −0.294 | −0.241 | −0.133 |
| Zn | −0.307 | −0.033 | −0.186 |
| As | **0.540** | **−0.687** | 0.311 |
| Ba | **0.531** | **0.466** | **−0.431** |
| Cd | **0.946** | −0.052 | −0.162 |
| Cr | **0.507** | −0.292 | −0.162 |
| Mo | **0.951** | −0.057 | −0.155 |
| Ni | −0.272 | −0.200 | −0.002 |
| Se | **0.766** | 0.113 | 0.159 |
| Sr | **0.772** | **0.498** | −0.179 |
| Pb | −0.279 | **−0.626** | **−0.502** |
| U | **0.626** | 0.146 | 0.300 |
| V | **0.551** | **−0.763** | −0.149 |
| W | **0.692** | **−0.552** | 0.224 |
| Eigenvalue | 11.5 | 4.75 | 2.70 |
| Variance (%) | 39.50 | 16.72 | 9.32 |
| Cumulative (%) | 39.50 | 56.22 | 65.54 |



Fig. 5. PCA biplots for the first two components (PC1 and PC2) explaining 39.50% and 16.72% of the total variability contained in the analysed variables, respectively. The figure a) shows the variables which contribute the most to the formation of PC1 and PC2 and depicts correlations between the variables. The figure b) shows groundwater sources (n = 28) with similar physicochemical parameters. The labels next to the points are sample identities, while their colour code is based on the description of surface lithology for their location (as per Fig. 2).

The lowest levels of these PTEs were in the sources located on the southern flank and partly in the southwest, in areas closer to Arusha City. Zones of lower Mo and U concentrations were also observed at higher elevations on the northwest and northeast flanks (Fig. 7).

From the distribution maps it could be further seen that the sources with elevated concentrations of measured parameters and PTEs are in the areas covered by debris avalanche deposits in the northeast, and volcanic ash or alluvial deposits in the southwest (Figs. 2, 6 and 7). In turn, water sources characterised by lower concentrations are associated with lava flows, which cover large part of the northern and southern flanks.

## 5. Discussion

### 5.1. Groundwater quality and human exposure to PTEs in the study area

The properties and quality of the groundwater in the Mt. Meru area have been reported in previous investigations mainly with respect to high F⁻, Na, K and HCO₃⁻ concentrations (e.g., Makoba and Muzuka, 2019; Chacha et al., 2018; Ghiglieri et al., 2012). These studies established that the water chemistry in the area is largely controlled by the local geology, whereby the enrichment of these ions in the water is attributed to weathering of volcanic rocks and related cycles of evaporation-precipitation. Given that the dominant water type in the area, NaHCO₃, is generally associated with high concentrations of other naturally occurring PTEs (Mariño et al., 2020; Rango et al., 2013; Reimann et al., 2003), this study focused on determining their levels to assess the potential health hazards to local communities that extend beyond the known F⁻ issues.

### 5.1.1. PTEs exceeding the drinking water guidelines

Our results revealed the presence of elevated concentrations of Mo (> 70 μg/L) and U (> 30 μg/L) (Fig. 4) in five (out of 48) samples,

including two adjacent springs (MW23 and MW24) and one well (MW20) with its associated tap system (MW21) in the northeast, and one tap water (MW49), with an unknown source, on the southwestern flank (Fig. 7). Comparably high concentrations of both Mo and U have been previously reported in the EARV groundwaters in Ethiopia (up to 450 μg/L for Mo and 70 μg/L U) by Rango et al. (2013, 2012, 2010)), but also in other volcanic regions across the world (e.g., in Italy, USA, Argentina) with varying aquifer lithology (e.g., Cidu et al., 2021; Coyte and Vengosh, 2020; Cinti et al., 2015; Nicolli et al., 2012; Bundschuh et al., 2004). To our knowledge, this is the first time their concentrations were determined in the groundwater sources located in the Arusha region. The sources of Mo and U-bearing groundwater in the study area are, furthermore, characterised by elevated concentrations of F⁻ (> 4 mg/L), Na (> 200 mg/L), K (> 50 mg/L) and high levels of TDS (> 1200 mg/L; Appendix 1) which are likely to make the water less desirable to consume. During site visits, the locals confirmed that these sources are generally not being used for drinking due to their 'saltiness', but occasionally for domestic purposes (MW20/21 and MW49) and keeping livestock (MW23 and W24).

High concentrations of U (ranging between 37 and 48 μg/L) were also found in seven other samples from sources located in the western and southwestern flanks (Fig. 7), including six wells (MW41, MW42, MW43, MW44, MW46 and MW50) and one spring (MW47). Most of these sources had high concentrations of Na (> 200 mg/L), variable concentrations of F⁻ (3–14 mg/L) and TDS levels ranging between 700 and

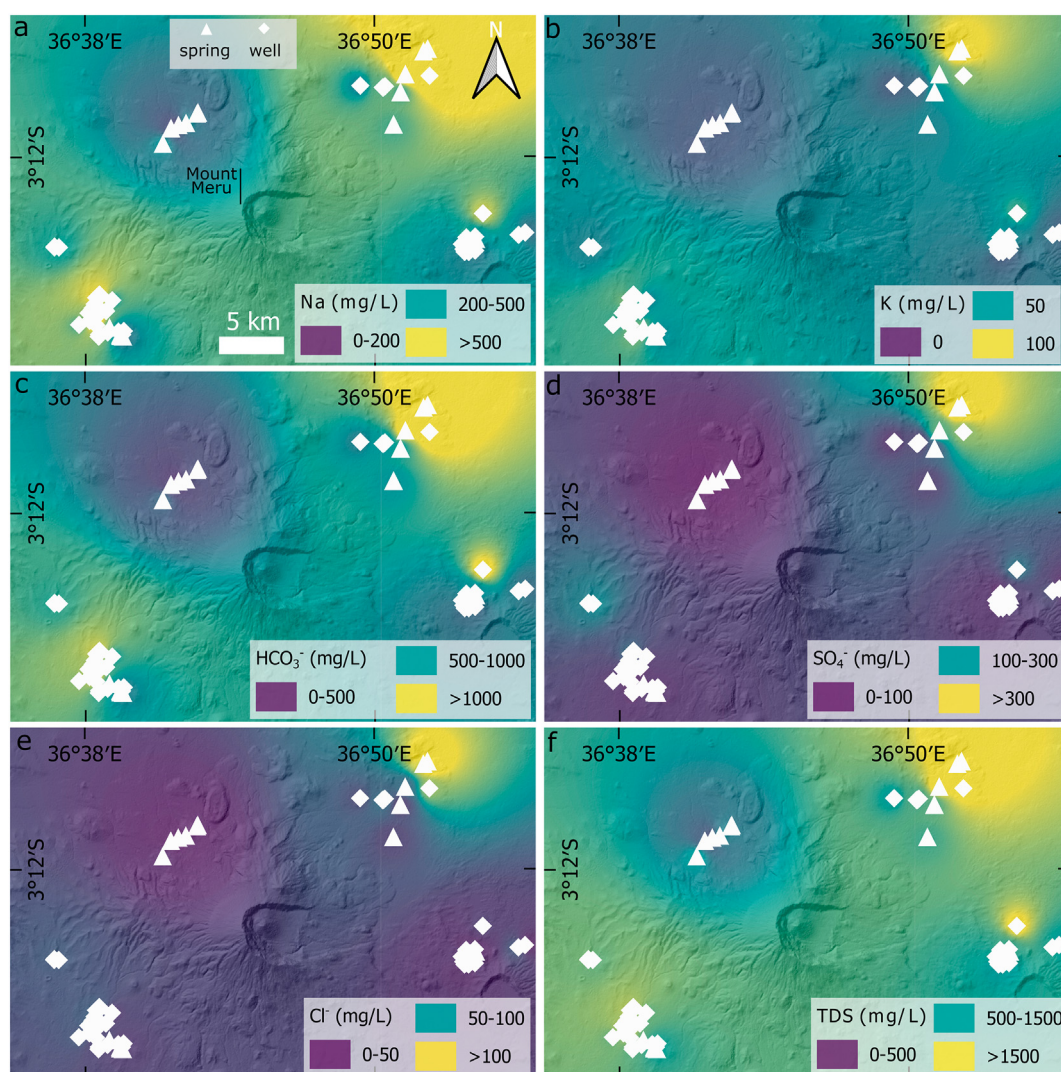**Fig. 6.** Spatial variation of a) sodium (Na$^+$), b) potassium (K$^+$), c) bicarbonate ion (HCO$_3^-$), d) sulphates (SO$_4^{2-}$), e) chloride (Cl$^-$) and f) total dissolved solids (TDS), in groundwater sources (springs - triangles and wells - diamonds) on the flanks of Mt. Meru. The maps show the IDW interpolation for 62 sampling points based on the data from Bennett et al. (2021).

1000 mg/L (Appendix 1). Based on the information collected in the field, these sources are used for domestic purposes including drinking and cooking.

*5.1.2. Presence of other naturally occurring PTEs*

Concentrations of other measured PTEs (As, Ba, Cd, Cr, Cu, Fe, Mn, Ni, Pb, Se, Sr) were found to be well within the recommended TBS and WHO health-based limits (Table 1, Figs. 3 and 4). Co-occurrence of elevated F$^-$ and As ($> 10\,\mu$g/L), in association with materials of volcanic origin, has been widely reported in the EARV and across the globe (Ligate et al., 2021; Bundschuh et al., 2021; Ahoulé et al., 2015; Kumar et al., 2016, 2020; Bhattacharya et al., 2006). Recently, it has been observed in some of the springs on the south-eastern flank of Mt. Meru volcano (Malago et al., 2020), however, concentrations of As measured in our samples were below 5 μg/L (Table 1). Moreover, Malago et al. (2020) reported high concentrations of Pb ($> 10\,\mu$g/L) in the same cluster of samples characterised by high As, however, the maximum Pb concentration measured in this study was much lower (1.1 μg/L; Table 1). We did observe higher average concentrations of Pb (0.2 μg/L) and Zn (23.5 μg/L) in tap water relative to analysed wells and springs (Fig. 3 and Fig. 4). This can possibly result from corrosion and/or interaction of water with Pb- and Zn-bearing materials used in the plumbing system

(pipes and fittings) distributing water in the area (Chowdhury et al., 2016).

In addition, plumbing materials could also be a potential source of other PTEs like V and W in water (Gerke et al., 2010), but their concentrations were largely comparable across the different sources (Fig. 4) thus indicating a common and likely natural origin. Their potential sources include a wide range of rock-forming minerals (e.g., plagioclase, fluorite, apatite, clay minerals) and volcanic glass, and they are often associated with metal-oxide compounds (Arnórsson and Óskarsson, 2007; Seiler et al., 2005). As safe levels are not yet established, V and W concentrations are not regulated, but based on some of the proposed limiting values and those generally found in groundwaters (Wright and Belitz, 2010; Steenstra et al., 2020; Hobson et al., 2020), the concentrations observed in the studied samples can be characterised as high. It is worth noting that both V and W are emerging elements of interest in research due to increasing health concerns over the possible adverse effects of their ingestion in drinking water (Imtiaz et al., 2015; Lemus and Venezia, 2015). The human health effects from exposure are not well known, but there is increasing evidence indicating that they can accumulate in, and be toxic to, plants and animals (Steenstra et al., 2020; Imtiaz et al., 2015). Nearly 63% ($n = 30$) of analysed samples
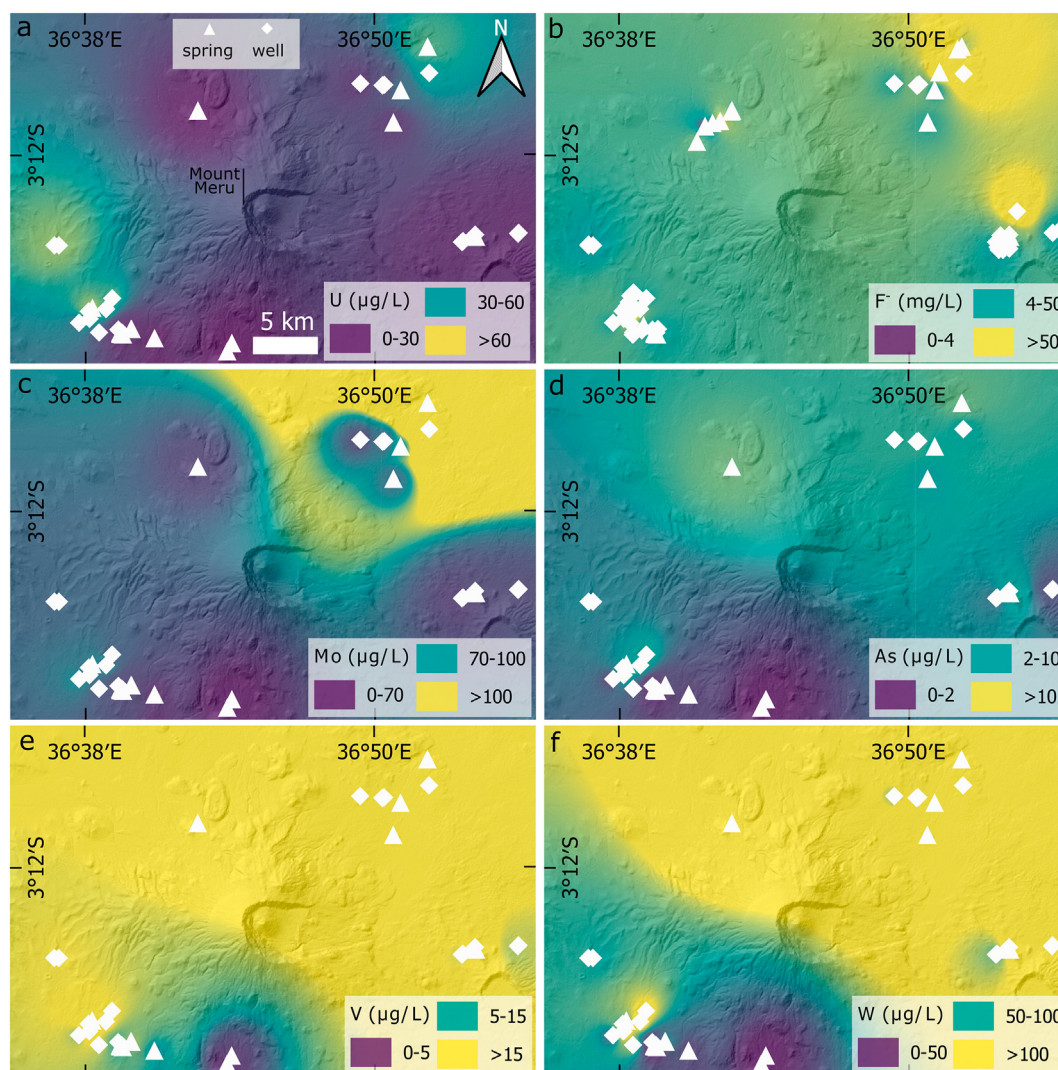
**Fig. 7.** Spatial distribution of a) uranium (U), b) fluoride (F-), c) molybdenum (Mo), d) arsenic (As), e) vanadium (V) and f) tungsten (W), in groundwater sources (springs - triangles and wells - diamonds) on the flanks of Mt. Meru. The maps show the IDW interpolation for 37 points sampled in the course of this study, except for fluoride which was based on data from Bennett et al. (2021) for 62 points.

contained more than 50 μg/L of W while 46% (n = 22) of samples had more than 15 μg/L of V (Appendix 1).

*5.1.3. Human health risk posed by elevated PTEs in groundwater sources*

Estimated HQ values for the sources described in Section 5.1.1, with high concentrations of Mo (> 70 μg/L) and U (> 30 μg/L), indicated that such concentrations of Mo and U are not safe for consumption for either children or adults (Appendix 2). This implies that continued drinking of water from these sources may pose a serious health risk. In general, the evidence on human health effects from exposures to high doses of Mo and U from drinking water is limited, but both have been linked with adverse health conditions (Smedley and Kinniburgh, 2017; Keith et al., 2013). Prolonged exposure to Mo has been associated with fatigue, lack of appetite, liver dysfunction, joint pain and tremor (Smedley and Kinniburgh, 2017), whereas exposure to U was shown to increase risk of kidney damage and possibly interference with normal bone functions (Ansoborlo et al., 2015; Arzuaga et al., 2015).

Overall, our analyses showed that poor water quality and elevated F⁻ (> 1.5 mg/L) in the local groundwater is in some instances coupled with high content of other PTEs (*e.g.*, Mo, U, V and W). This is concerning since the effects of exposure to multiple PTEs may be synergistic or antagonistic and the effective toxicity might be increased even if they are present in levels lower than the regulatory limits for an individual

element (Chowdhury et al., 2016; Mitchell et al., 2011). Moreover, it is worth nothing that the local standards for safe levels for most of the constituents in drinking water are higher than those recommended by the WHO (Table 1). Local guidelines also do not yet regulate the levels of elements such as K, Na, Al, Mo, Ni, Sr, U, V and W.

*5.2. Spatial distribution of PTEs and their association with other water quality parameters*

The co-occurrence of F⁻ with other PTEs such as Mo, U and V in the study area is consistent with findings of previous hydrochemical studies in the EARV and other volcanic areas, which suggested their mobilization is directly linked to alkaline pH conditions combined with NaHCO₃ hydrochemical facies of water (*e.g.*, Rango et al., 2013; Reimann et al., 2003; Bird et al., 2020; Mariño et al., 2020; Alcaine et al., 2020). However, there was no consistent pattern or relationship between elevated levels of PTEs with high concentrations of F⁻ (> 4 mg/L), which are widely distributed across the study area (Fig. 7, Bennett et al. (2021)).

*5.2.1. Areas of high PTE concentrations/poor groundwater quality*

Our spatial analyses showed that the water sources with concerning levels of PTEs (Mo and U) are located on the northeast and southwest

flanks of the volcano (Fig. 7). The cluster of samples in the northeast (well MW20, and springs MW23 and MW24) corresponds to the cluster of samples on the biplot (quadrant 4 in Fig. 5b) characterised by the highest concentrations of water-dominant parameters (TDS, Na, K, $HCO_3^-$, $Cl^-$, $SO_4^{2-}$) and high $F^-$ concentrations (> 20 mg/L). Moderate to strong correlation of these parameters with U and Mo, respectively (Fig. 5b) indicate a possible common origin (*i.e.*, source materials) and that their occurrence in the groundwater is influenced, at least in part, by the same processes.

Prevalent deposits in this area are debris avalanche deposits (Fig. 2), *i.e.*, brecciated volcanic material supported by a fine matrix emplaced by a large landslide (Delcamp et al., 2017). The volcanic clasts in these deposits are rich in Na-, K- and $F^-$-bearing minerals such as sanidine, nepheline and (fluor)apatite (Ghiglieri et al., 2012). The topography of this area (*i.e.*, lower elevation, distance from the recharge zone in the centre of Mt. Meru) favours the conditions that lead to high ion concentrations in these water sources, which include longer water-rock interaction time, high evaporation and low precipitation (Makoba and Muzuka, 2019). Higher temperature and possible introduction of $CO_2$ from volcanic and geothermal activities are also considered additional factors favouring high concentrations in the waters, both locally and in the EARV, in general (Makoba and Muzuka, 2019; Rango et al., 2010).

It is likely that similar seasonal conditions (high temperature, low precipitation) at the windward side and interaction of water with voluminous volcanic ash and alluvial deposits influence the occurrence of high U in the sources located in the southwest at the base of the volcano (Figs. 2 and 7). Due to their fine-grained nature, these deposits are particularly reactive and susceptible to weathering and consequently contribute to high concentrations of dissolved ions in the groundwater (Makoba and Muzuka, 2019; Ghiglieri et al., 2012). The most plausible mechanisms controlling the release of PTEs, specifically oxyanion-forming elements such as U, Mo, As, V and W, were found to be dissolution of volcanic glass and (de)sorption reactions involving weathering products like metal oxides (Al, Fe or Mn) and clay minerals (Mariño et al., 2020; Smedley and Kinniburgh, 2017; Rango et al., 2013; Bundschuh et al., 2013). Possible differences in the content of such phases across the different deposits, as well as their sensitivity to changes in water pH and redox conditions, may explain the observed spatial variation in concentrations of U and Mo in analysed wells and springs (Fig. 7).

*5.2.2. Areas with safe(r) levels of PTEs in the groundwater sources*

Lower levels of these PTEs were found in the sources located on the southern flank and partly in the southwest, in areas closer to Arusha (Fig. 7). Based on the grouping of some of these water sources on the biplot (quadrant 2 in Fig. 5b), it can be observed that they are characterised by low concentrations of dominant parameters and relatively high $NO_3^-$ (> 10 mg/L). The source of $NO_3^-$ is most likely anthropogenic, due to proximity to urbanised areas and activities such as agriculture (*i.e.*, application of fertilizers) and/or domestic waste and wastewater disposal (Elisante and Muzuka, 2016; Ward et al., 2018). With regards to the lithology, this area is largely covered by nephelinitic or phonolitic lava deposits and volcanic breccias and tuffs (Fig. 2). Aquifers hosted in these rocks have been associated with a low release of fluoride due to their high permeability, which reduces the residence time of groundwater, but also because of their resistivity to weathering and associated absence of secondary products or salty deposits (Ghiglieri et al., 2010; Makoba and Muzuka, 2019). Moreover, lava flows overlie the central part of Mt. Meru and a large part of the lower northern flanks, where zones of lower Mo and U concentrations were also observed (Fig. 7). Water sources in these areas are in proximity to the recharge zone at higher elevations (central Mt. Meru) which leads to shorter water-rock interaction time relative to other areas. It is reasonable to assume that the described properties and processes also affect the release of other ions including investigated PTEs to the groundwater.

Apart from the described distinct sample clusters in the study area, our analysis showed that other investigated water sources vary in their chemical signatures (quadrant 3 in Fig. 5b), which suggests that their PTE concentrations in the groundwater are probably influenced by a combination of discussed factors and/or processes. Spatial distribution of these sources and associated PTE levels is rather erratic. However, in line with the main observations, the sources with lowest TDS and concentrations of other measured PTEs, specifically of As, V and W, were springs in the southern flanks of the volcano (Fig. 7). The distribution maps also reflect the observed correlation between these elements, and their negative association with the occurrence of $NO_3^-$ in the water (Fig. 5a). Similar low-level characteristics, with the exception of V and W concentration, define water from the spring sampled in the northern flank at the highest elevation visited in the course of this study (MW12 at 2075 m a.s.l) which is probably a source of sampled tap systems in the area at a lower elevation (MW13, and possibly MW14 and MW15). While all other analysed PTEs were within the regulated/acceptable health limits, concentrations of V and W in these sources were above 15 μg/L and 50 μg/L, respectively (Appendix 1). Although the maps indicate a wide distribution of V and W across the studied area, this observation should be taken with reservation, specifically for the northern and eastern flanks at higher elevation, as the inclusion of spring MW12 in the spatial analysis (*i.e.*, its distance from other sources) affected the interpolation (Fig. 7). Sampling and analysis of additional water sources in the central parts of Mt. Meru would help to refine the interpolation, which was not possible during the course of this field campaign due to the restricted access to their location (within the Arusha National Park).

## 6. Conclusions

The findings of this study confirmed that the local geochemical processes and conditions in the Mt. Meru area can mobilise PTEs other than $F^-$ from the local aquifers and, in this way, potentially lead to natural groundwater contamination by elements such as Mo, U, V and W. The results showed that majority of analysed elements (Al, As, Ba, Cd, Cr, Cu, Fe, Mn, Ni, Se, Sr, Pb, and Zn) are within the acceptable limits for drinking purpose in sampled wells, springs and tap systems, suggesting that there is no immediate health risk associated with these PTEs. However, some of the water samples were found to exceed the WHO tolerance limit for drinking water for U (> 30 μg/L) and Mo (> 70 μg/L). The sample analysis also revealed that in some of the collected samples, the concentrations of TDS, Na and K exceed the permissible limits.

Discovery of elevated levels of multiple PTEs (*i.e.*, Mo, U, V, W) in some of the analysed sources is of health concern especially considering the existing $F^-$ issues afflicting the local communities, but also the water scarcity in the area which often forces people to consume any existing water resource. The present data were too limited to appropriately assess the cumulative risk of exposure to multiple PTEs; instead, we estimated the individual risk posed by Mo and U, and we only considered exposures to drinking water. Although water is a likely primary source of potential excess intake of PTEs, a complete risk calculation should include other sources of intake such as food as well as other exposure routes (dermal and inhalation). The findings of the present study thus suggest a need for further detailed studies on the occurrence and levels of these PTEs in the area.

The concerning levels of major parameters and PTEs were found in areas covered with debris avalanche deposits on the northeast flank, and volcanic ash and alluvial deposits on the southwest flanks of the volcano. From this and past investigations, it is relatively clear that the interaction of groundwater with these deposits is the most influential factor regulating the concentrations of investigated PTEs across the different water sources. Further investigation would be required to assess possible seasonal differences in PTE concentrations, as their mobility can be affected by associated variations in hydrochemical parameters. The areas of high concentrations would also benefit from detailed

mineralogical studies to complement the current findings and provide a better understanding on the sources of Mo and U. The occurrence of 'emerging contaminants' such as V and W may also require additional attention.

In conclusion, this study highlights the need to extend the range of elements monitored in the regional groundwater and make a more routine measurement of PTEs such as U and Mo, at least on a reconnaissance scale. This will be important to ensure drinking water safety and effective water management measures for the growing local population and associated expansion of agricultural activities and increased water demand for domestic purposes. The findings may also have implications for other regions in the EARV and areas with similar geology and climate.

Supplementary data to this article can be found online at https://doi.org/10.1016/j.scitotenv.2021.150487.

## Data availability

The datasets used and/or analysed during the current study are submitted as Supplementary Information.

## CRediT authorship contribution statement

**Ines Tomašek:** Conceptualization, Methodology, Investigation, Formal analysis, Visualization, Writing – original draft. **Hassina Mouri:** Conceptualization, Writing – review & editing. **Antoine Dille:** Formal analysis, Visualization, Writing – review & editing. **George Bennett:** Investigation, Writing – review & editing. **Prosun Bhattacharya:** Writing – review & editing. **Natacha Brion:** Investigation. **Marc Elskens:** Funding acquisition, Supervision, Writing – review & editing. **Karen Fontijn:** Writing – review & editing. **Yue Gao:** Funding acquisition, Resources, Methodology. **Patrick Kirita Gevera:** Formal analysis, Writing – review & editing. **Julian Ijumulana:** Writing – review & editing. **Mary Kisaka:** Investigation, Writing – review & editing. **Martine Leermakers:** Investigation, Writing – review & editing. **Ceven Shemsanga:** Conceptualization, Investigation. **Kristine Walraevens:** Conceptualization, Writing – review & editing. **Joanna Wragg:** Conceptualization, Writing – review & editing. **Matthieu Kervyn:** Conceptualization, Resources, Funding acquisition, Project administration, Supervision, Writing – review & editing.

## Declaration of competing interest

The authors declare that they have no known competing financial interests or personal relationships that could have appeared to influence the work reported in this paper.

## References

Ahoulé, D.G., Lalanne, F., Mendret, J., Brosillon, S., Maïga, A.H., 2015. Arsenic in African waters: a review. Water Air Soil Pollut. 226, 302.

Alcaine, A.A., Schulz, C., Bundschuh, J., Jacks, G., Thunvik, R., Gustafsson, J.-P., Mörth, C.-M., Sracek, O., Ahmad, A., Bhattacharya, P., 2020. Hydrogeochemical controls on the mobility of arsenic, fluoride and other geogenic co-contaminants in the shallow aquifers of northeastern La Pampa Province in Argentina. Sci. Total Environ. 715, 136671.

Ansoborlo, E., Lebaron-Jacobs, L., Prat, O., 2015. Uranium in drinking-water: a unique case of guideline value increases and discrepancies between chemical and radiochemical guidelines. Environ. Int. 77, 1–4.

Arnórsson, S., Óskarsson, N., 2007. Molybdenum and tungsten in volcanic rocks and in surface and< 100 C ground waters in Iceland. Geochim. Cosmochim. Acta 71 (2), 284–304.

Arzuaga, X., Gehlhaus, M., Strong, J., 2015. Modes of action associated with uranium induced adverse effects in bone function and development. Toxicol. Lett. 236, 123–130.

Bennett, G., Van Reybrouck, J., Shemsanga, C., Kisaka, M., Tomašek, I., Fontijn, K., Kervyn, M., Walraevens, K., 2021. Hydrochemical characterisation of high-fluoride groundwater and development of a conceptual groundwater flow model using a combined hydrogeological and Hydrochemical approach on an active volcano: Mount Meru, northern Tanzania. Water 13 (16), 2159.

Bhattacharya, P., Claesson, M., Bundschuh, J., Sracek, O., Fagerberg, J., Jacks, G., ... Thir, J.M., 2006. Distribution and mobility of arsenic in the Rio Dulce alluvial aquifers in Santiago del Estero Province, Argentina. Sci. Total Environ. 358 (1–3), 97–120.

Bird, K.S., Navarre-Sitchler, A., Singha, K., 2020. Hydrogeological controls of arsenic and uranium dissolution into groundwater of the pine ridge reservation, South Dakota. Appl. Geochem. 114, 104522.

Bundschuh, J., Farias, B., Martin, R., Storniolo, A., Bhattacharya, P., Cortes, J., ... Albouy, R., 2004. Groundwater arsenic in the Chaco-Pampean plain, Argentina: case study from robles county, Santiago del Estero province. Appl. Geochem. 19 (2), 231–243.

Bundschuh, J., Maity, J.P., Nath, B., Baba, A., Gunduz, O., Kulp, T.R., Jean, J.-S., Kar, S., Yang, H.-J., Tseng, Y.-J., 2013. Naturally occurring arsenic in terrestrial geothermal systems of western Anatolia, Turkey: potential role in contamination of freshwater resources. J. Hazard. Mater. 262, 951–959.

Bundschuh, J., Maity, J.P., Mushtaq, S., Vithanage, M., Seneweera, S., Schneider, J., Bhattacharya, P., Khan, N.I., Hamawand, I., Guilherme, L.R., 2017. Medical geology in the framework of the sustainable development goals. Sci. Total Environ. 581, 87–104.

Bundschuh, J., Armienta, M.A., Morales-Simfors, N., Alam, M.A., Lopez, D.L., Delgado Quezada, V., ... Ahmad, A., 2021. Arsenic in Latin America: new findings on source, mobilization and mobility in human environments in 20 countries based on decadal research 2010-2020. Crit. Rev. Environ. Sci. Technol. 51 (16), 1727–1865.

Chacha, N., Njau, K.N., Lugomela, G.V., Muzuka, A.N., 2018. Hydrogeochemical characteristics and spatial distribution of groundwater quality in Arusha well fields, northern Tanzania. Appl Water Sci 8, 118.

Chowdhury, S., Mazumder, M.J., Al-Attas, O., Husain, T., 2016. Heavy metals in drinking water: occurrences, implications, and future needs in developing countries. Sci. Total Environ. 569, 476–488.

Cidu, R., Biddau, R., Frau, F., Wanty, R.B., Naitza, S., 2021. Regional occurrence of aqueous tungsten and relations with antimony, arsenic and molybdenum concentrations (Sardinia, Italy). J. Geochem. Explor. 106846.

Cinti, D., Poncia, P.P., Brusca, L., Tassi, F., Quattrocchi, F., Vaselli, O., 2015. Spatial distribution of arsenic, uranium and vanadium in the volcanic-sedimentary aquifers of the Vicano–Cimino Volcanic District (Central Italy). J. Geochem. Explor. 152, 123–133.

Coyte, R.M., Vengosh, A., 2020. Factors controlling the risks of co-occurrence of the redox-sensitive elements of arsenic, chromium, vanadium, and uranium in groundwater from the eastern United States. Environ. Sci. Technol. 54 (7), 4367–4375.

Davies, T.C., 2008. Environmental health impacts of east African rift volcanism. Environ. Geochem. Health 30, 325–338.

Delcamp, A., Kervyn, M., Benbakkar, M., Kwelwa, S., Peter, D., 2017. Large volcanic landslide and debris avalanche deposit at Meru, Tanzania. Landslides 14, 833–847.

Edmunds, W.M., Smedley, P.L., 1996. Groundwater geochemistry and health: an overview. Geol. Soc. Lond., Spec. Publ. 113, 91–105.

Elisante, E., Muzuka, A.N., 2016. Assessment of sources and transformation of nitrate in groundwater on the slopes of Mount Meru, Tanzania. Environ. Earth Sci. 75, 277.

Fordyce, F.M., 2013. Selenium deficiency and toxicity in the environment. Essentials of Medical Geology. Springer, pp. 375–416.

Gerke, T.L., Scheckel, K.G., Maynard, J.B., 2010. Speciation and distribution of vanadium in drinking water iron pipe corrosion by-products. Sci. Total Environ. 408, 5845–5853.

Gevera, P., Mouri, H., 2018. Natural occurrence of potentially harmful fluoride contamination in groundwater: an example from Nakuru County, the Kenyan Rift Valley. Environ. Earth Sci. 77, 365.

Gevera, P., Mouri, H., Maronga, G., 2019. Occurrence of fluorosis in a population living in a high-fluoride groundwater area: Nakuru area in the central Kenyan Rift Valley. Environ. Geochem. Health 41, 829–840. https://doi.org/10.1007/s10653-018-0180-2.

Gevera, Cave, M., Dowling, K., Gikuma-Njuru, P., Mouri, H., 2020. Naturally occurring potentially harmful elements in groundwater in Makueni County, south-eastern Kenya: effects on drinking water quality and agriculture. Geosciences 10, 62.

Ghiglieri, G., Balia, R., Oggiano, G., Pittalis, D., 2010. Prospecting for safe (low fluoride) groundwater in the eastern African rift: the Arumeru District (northern Tanzania). Hydrol. Earth Syst. Sci. 14, 1081–1091.

Ghiglieri, G., Pittalis, D., Cerri, G., Oggiano, G., 2012. Hydrogeology and hydrogeochemistry of an alkaline volcanic area: the NE Mt. Meru slope (East African Rift-Northern Tanzania). Hydrol. Earth Syst. Sci. 16.

Gilman, A.P., Villeuve, D.C., Secours, V.E., Yagminas, A.P., Tracy, B.L., Quinn, J.M., Valli, V.E., Willes, R.J., Moss, M.A., 1998. Uranyl nitrate: 28-day and 91-day toxicity studies in the Sprague-Dawley rat. Toxicol. Sci. 41, 117–128.

Hobson, C., Kulkarni, H.V., Johannesson, K.H., Bednar, A., Tappero, R., Mohajerin, T.J., Sheppard, P.R., Witten, M.L., Hettiarachchi, G.M., Datta, S., 2020. Origin of tungsten and geochemical controls on its occurrence and mobilization in shallow sediments from Fallon, Nevada, USA. Chemosphere 260, 127577.

Ijumulana, J., Ligate, F., Bhattacharya, P., Mtalo, F., Zhang, C., 2020. Spatial analysis and GIS mapping of regional hotspots and potential health risk of fluoride concentrations in groundwater of northern Tanzania. Sci. Total Environ. 139584.

Ijumulana, J., Ligate, F., Irunde, R., Bhattacharya, P., Maity, J.P., Ahmad, A., Mtalo, F., 2021. Spatial uncertainties in fluoride levels and health risks in endemic fluorotic regions of northern Tanzania. Groundw. Sustain. Dev. 14, 100618.

Imtiaz, M., Rizwan, M.S., Xiong, S., Li, H., Ashraf, M., Shahzad, S.M., Shahzad, M., Rizwan, M., Tu, S., 2015. Vanadium, recent advancements and research prospects: a review. Environ. Int. 80, 79–88.

Keith, S., Faroon, O., Roney, N., Scinicariello, F., Wilbur, S., Ingerman, L., Llados, F., Plewak, D., Wohlers, D., Diamond, G., 2013. Toxicological profile for uranium.

Kimambo, V., Bhattacharya, P., Mtalo, F., Mtamba, J., Ahmad, A., 2019. Fluoride occurrence in groundwater systems at global scale and status of defluoridation–state of the art. Groundw. Sustain. Dev. 9, 100223.

Kisaka, M., Fontijn, K., Shemsanga, C., Tomašek, I., Gaduputi, S., Debaille, V., Delcamp, A., Kervyn, M., 2021. The late Quarternary eruptive history of Meru volcano, northern Tanzania. J. Volcanol. Geotherm. Res. 417, 1–14 107314.

Kitalika, A.J., Machunda, R.L., Komakech, H.C., Njau, K.N., 2018. Fluoride variations in rivers on the slopes of Mount Meru in Tanzania. J. Chem. 2018.

Kumar, M., Das, N., Goswami, R., Sarma, K.P., Bhattacharya, P., Ramanathan, A.L., 2016. Coupling fractionation and batch desorption to understand arsenic and fluoride co-contamination in the aquifer system. Chemosphere 164, 657–667.

Kumar, M., Goswami, R., Patel, A.K., Srivastava, M., Das, N., 2020. Scenario, perspectives and mechanism of arsenic and fluoride co-occurrence in the groundwater: a review. Chemosphere 126126.

Lemus, R., Venezia, C.F., 2015. An update to the toxicological profile for water-soluble and sparingly soluble tungsten substances. Crit. Rev. Toxicol. 45, 388–411.

Ligate, F., Ijumulana, J., Ahmad, A., Kimambo, V., Irunde, R., Mtamba, J.O., ... Bhattacharya, P., 2021. Groundwater resources in the East African Rift Valley: Understanding the geogenic contamination and water quality challenges in Tanzania. Sci. Afr. 13, 1–14 e00831.

Makoba, E., Muzuka, A.N., 2019. Water quality and hydrogeochemical characteristics of groundwater around Mt. Meru, Northern Tanzania. Appl Water Sci 9, 120.

Malago, J., Makoba, E., Muzuka, A.N., 2017. Fluoride levels in surface and groundwater in Africa: a review. Am. J. Water Sci. Eng. 3, 1.

Malago, J., Makoba, E., Muzuka, A.N., 2020. Spatial distribution of arsenic, boron, fluoride, and lead in surface and groundwater in Arumeru District, Northern Tanzania. Fluoride 53.

Mariño, E.E., Ávila, G.T., Bhattacharya, P., Schulz, C.J., 2020. The occurrence of arsenic and other trace elements in groundwaters of the southwestern Chaco-Pampean plain, Argentina. J. S. Am. Earth Sci. 102547.

Mbabaye, G., Minja, R., Mtalo, F., Legonda, I., Mkongo, G., 2018. Fluoride occurrence in domestic water supply sources in Tanzania: a case of Meru district Arusha region. Tanz. J. Sci. 44, 72–92.

Mekonnen, K.N., Ambushe, A.A., Chandravanshi, B.S., Abshiro, M.R., McCrindle, R.I., 2012. Potentially toxic elements in some fresh water bodies in Ethiopia. Toxicol. Environ. Chem. 94, 1980–1994.

Mitchell, E., Frisbie, S., Sarkar, B., 2011. Exposure to multiple metals from groundwater—a global crisis: geology, climate change, health effects, testing, and mitigation. Metallomics 3, 874–908.

Mkungu, J., Machunda, R.L., Muzuka, A.N.N., 2014. Application of soil composition for inferring fluoride variability in volcanic areas of Mt. Meru, Tanzania. Int. J. Environ. Monitor. Analysis 2, 231.

Muhammad, S., Shah, M.T., Khan, S., 2011. Health risk assessment of heavy metals and their source apportionment in drinking water of Kohistan region, northern Pakistan. Microchem. J. 98, 334–343.

Nicolli, H.B., García, J.W., Falcón, C.M., Smedley, P.L., 2012. Mobilization of arsenic and other trace elements of health concern in groundwater from the Salí River Basin, Tucumán Province, Argentina. Environ. Geochem. Health 34 (2), 251–262.

Nwankwo, C.B., Hoque, M.A., Islam, M.A., Dewan, A., 2020. Groundwater constituents and trace elements in the basement aquifers of Africa and sedimentary aquifers of Asia: medical hydrogeology of drinking water minerals and toxicants. Earth Syst. Environ. 4, 369–384.

Ormachea Munoz, M., Wern, H., Johnsson, F., Bhattacharya, P., Sracek, O., Thunvik, R., Quintanilla, J., Bundschuh, J., 2013. Geogenic arsenic and other trace elements in the shallow hydrogeologic system of Southern Poopó Basin, Bolivian Altiplano. J. Hazard. Mater. 262, 924–940.

Quino Lima, I., Ramos Ramos, O.R., Ormachea Munoz, M., Quintanilla Aguirre, J., Duwig, C., Maity, J.P., Sracek, O., Bhattacharya, P., 2020. Spatial dependency of arsenic, antimony, boron and other trace elements in the shallow groundwater systems of the Lower Katari Basin, Bolivian Altiplano. Sci. Total Environ. 719, 137505.

Rahman, M.M., Dong, Z., Naidu, R., 2015. Concentrations of arsenic and other elements in groundwater of Bangladesh and West Bengal, India: potential cancer risk. Chemosphere 139, 54–64.

Rango, T., Bianchini, G., Beccaluva, L., Ayenew, T., Colombani, N., 2009. Hydrogeochemical study in the Main Ethiopian Rift: new insights to the source and enrichment mechanism of fluoride. Environ. Geol. 58, 109–118.

Rango, T., Bianchini, G., Beccaluva, L., Tassinari, R., 2010. Geochemistry and water quality assessment of central Main Ethiopian Rift natural waters with emphasis on source and occurrence of fluoride and arsenic. J. Afr. Earth Sci. 57, 479–491.

Rango, T., Kravchenko, J., Atlaw, B., McCornick, P.G., Jeuland, M., Merola, B., Vengosh, A., 2012. Groundwater quality and its health impact: an assessment of dental fluorosis in rural inhabitants of the Main Ethiopian Rift. Environ. Int. 43, 37–47.

Rango, T., Vengosh, A., Dwyer, G., Bianchini, G., 2013. Mobilization of arsenic and other naturally occurring contaminants in groundwater of the Main Ethiopian Rift aquifers. Water Res. 47, 5801–5818.

Reimann, C., Bjorvatn, K., Frengstad, B., Melaku, Z., Tekle-Haimanot, R., Siewers, U., 2003. Drinking water quality in the Ethiopian section of the East African Rift Valley I—data and health aspects. Sci. Total Environ. 311, 65–80.

Roberts, M.A., 2003. Geochemical and Volcanological Evolution of the Mt. Meru Region, Northern Tanzania. University of Cambridge.

Seiler, R.L., Stollenwerk, K.G., Garbarino, J.R., 2005. Factors controlling tungsten concentrations in ground water, Carson Desert, Nevada. Appl. Geochem. 20 (2), 423–441.

Smedley, P.L., Kinniburgh, D.G., 2017. Molybdenum in natural waters: a review of occurrence, distributions and controls. Appl. Geochem. 84, 387–432.

Steenstra, P., Strigul, N., Harrison, J., 2020. Tungsten in Washington State surface waters. Chemosphere 242, 125151.

Tchounwou, P.B., Yedjou, C.G., Patlolla, A.K., Sutton, D.J., 2012. Heavy metal toxicity and the environment. Molecular, Clinical and Environmental Toxicology. Springer, pp. 133–164.

Wang, S., Shi, X., 2001. Molecular mechanisms of metal toxicity and carcinogenesis. Mol. Cell. Biochem. 222, 3–9.

Ward, M.H., Jones, R.R., Brender, J.D., De Kok, T.M., Weyer, P.J., Nolan, B.T., Villanueva, C.M., Van Breda, S.G., 2018. Drinking water nitrate and human health: an updated review. Int. J. Environ. Res. Public Health 15, 1557.

WHO, 2003. Domestic water quantity, service level and health. Howard G. and J. Bartram, WHO/SDE/WSH/3.02.

WHO, 2017. Guidelines for drinking-water quality: first addendum to the fourth edition.

Wilkinson, P., Mitchell, J.G., Cattermole, P.J., Downie, C., 1986. Volcanic chronology of the Men–Kilimanjaro region, Northern Tanzania. J. Geol. Soc. 143, 601–605.

Wold, S., Esbensen, K., Geladi, P., 1987. Principal component analysis. Chemom. Intell. Lab. Syst. 2, 37–52.

Wright, M.T., Belitz, K., 2010. Factors controlling the regional distribution of vanadium in groundwater. Groundwater 48, 515–525.

Zimmermann, M.B., 2009. Iodine deficiency. Endocr. Rev. 30, 376–408.